Effect of disorder and lattice type on domain-wall motion in two dimensions

Belita Koiller,* Hong Ji,† and Mark O. Robbins
Department of Physics and Astronomy, Johns Hopkins University, Baltimore, Maryland 21218
(Received 16 January 1992)

We study the general problem of interface motion through a disordered medium taking as an example the random-field Ising model in two dimensions. Spins are placed on the sites of a square, triangular, or honeycomb array. Each interacts with a random local field from a bounded distribution. Growth of a domain through the array is driven by a uniform external magnetic field. When the random field strength is large, the domain of flipped spins forms a fractal percolationlike pattern. As the randomness decreases, there is a transition to compact two-dimensional growth with a faceted interface. In the square and triangular lattices there is a power-law divergence of a characteristic correlation length or fingerwidth at the transition. The exponents relating this divergence to the probabilities that local spin configurations are stable are found to be universal. In contrast, there is a discontinuous transition from fractal to faceted growth on the honeycomb lattice that occurs in the limit of zero randomness. We show that the problem of domain growth is related to a continuous family of bootstrap percolation models.

I. INTRODUCTION

Fluid invasion in porous media[1] and domain growth in disordered magnetic systems[2,3] are fundamental processes whose study has also provided a great deal of insight into more general growth problems. Both processes involve the motion of an interface between two phases through a disordered system. Other examples of this common phenomenon include phase segregation in gels[4] and spreading of fluids on dirty surfaces.[5,6] Recent work has shown that a number of novel critical transitions occur as the degree of disorder in the medium, the force driving the interface, and other physical properties are varied.[6–11] Of particular interest are changes in the morphology of the advancing interface from a self-similar fractal to a self-affine or faceted form as the effective degree of disorder decreases.

Theoretical and experimental studies of growth morphology in fluid invasion have focused on simple two-dimensional model systems such as thin glass bead packs[12,13] or networks of random-width ducts.[1,13] Early work on network models showed that invasion by nonwetting and wetting fluids was very different.[1] Invasion by a nonwetting fluid produced fractal patterns characteristic of the invasion percolation model,[14] while invasion by a more wetting fluid could produce smooth faceted interfaces.[1] We have recently modeled invasion of square network models as a function of both the degree of disorder and the contact angle θ of the invading fluid.[10] We found a transition from invasion percolation at high disorder or contact angle (invading fluid less wetting) to faceted growth at low disorder or contact angle. This transition is associated with a diverging coherence length and reflects a growing correlation in the advance of neighboring segments of the interface. Decreasing the contact angle increases the interaction between neighboring segments and increasing the degree of disorder suppresses these interactions. The exponent relating the divergence of the coherence length to changes in contact angle or disorder is not universal.[10]

A very similar transition has been found in domain growth in the random-field Ising model on a square lattice.[9] In particular, growth is percolationlike when the amplitude of the random fields is large and becomes faceted as the amplitude decreases. There is a diverging correlation length at the critical amplitude. These similarities are evidence of the strong analogies between domain growth and fluid invasion.[3,6,9] The domains of up and down spins correspond to the two fluid phases, and an applied magnetic field, which favors up spins, plays the role of the pressure driving invasion.

In the present paper, we further explore the morphology of growth in two-dimensional models by systematically investigating different lattices and distributions of disorder. The random-field Ising model is adopted due to its analogy and relative simplicity with respect to models of fluid invasion. We find a transition from fractal to faceted growth on the triangular lattice, which is very similar to that on the square lattice. Indeed, we show that there is universal scaling of the coherence length on the two lattices. However, the universal behavior is in terms of variations in the probability of stability of local spin configurations rather than in the amplitude of the disorder. Invasion of the honeycomb array is entirely different. Any finite value of the randomness leads to a fractal invasion pattern. The fingerwidth diverges discontinuously at zero randomness.

We also show that domain growth can be related to generalized bootstrap or diffusion percolation models,[15,16] in which the local environment has a certain probability of changing the state of a site. Our results provide new information about diffusion percolation on

the honeycomb array and are consistent with results on the square and triangular lattices.

The Hamiltonian and growth model used in our study are described in the following section. Section III presents results on changes in growth morphology with disorder, and Sec. IV describes the relation between domain growth and correlated percolation models. The final section gives a summary and conclusions.

II. DESCRIPTION OF GROWTH MODEL

The Hamiltonian and rules for domain-wall motion are described in detail in Ref. 9. That paper also motivates and justifies the rules in terms of the analogy to fluid invasion. We briefly review the model here.

Ising spins $s_i = \pm 1$ are placed on each site i of a two-dimensional (2D) array. Their Hamiltonian, in units of the exchange coupling, is

$$\mathcal{H} = -\sum_{\langle i,j \rangle} s_i s_j - \sum_i (h_i + H) s_i \ . \tag{1}$$

The first term is a nearest-neighbor spin-spin exchange interaction. The second term describes the interaction of each spin with the sum of the local random field h_i and a uniform external magnetic field H. Values of h_i are generated randomly following some probability distribution function $P(h)$, which we take to be continuous, symmetric, and bounded between $\pm\Delta$. The degree of randomness is characterized by the magnitude of Δ. Three forms for P were studied: uniform, $P(h) = (2\Delta)^{-1}$; linear, $P(h) = (\Delta - |h|)\Delta^{-2}$; and cosinusoidal, $P(h) = (\pi/4\Delta)\cos(\pi h/2\Delta)$.

We present results for square, triangular, and honeycomb arrays. Each array contains L^2 spins with L ranging from 30 to 4000. Measuring length in units of the nearest-neighbor distance, the resulting array dimensions are $L \times L$ for the square lattice, $L \times (\sqrt{3}/2)L$ for the triangular lattice, and $(\sqrt{3}/2)L \times 2L$ for the honeycomb array. Periodic boundary conditions are imposed in the horizontal direction. Between 20 and 100 different realizations of the random fields assigned to each site were studied for each type of lattice, form of $P(h)$, and value of L and Δ to obtain reliable average quantities.

Spins at the bottom edge of the simulation array are originally "flipped" ($s = +1$), while all other spins are "unflipped" ($s = -1$). The initial interface or domain wall is therefore a horizontal line. To mimic the process of fluid invasion, growth occurs at zero temperature and *only spins at the interface are allowed to flip.* The zero-temperature condition and single-spin-flip dynamics[17] have important implications for the phase diagrams discussed below. In particular, there is no ordered phase at finite temperature in the 2D random-field Ising model.[18] However, the thermal activation barriers for fluid invasion and other macroscopic growth processes are so large that the zero-temperature approximation is accurate on experimental time scales.

An interface spin is flipped when this lowers the total energy of the system. If there is more than one unstable spin on the interface, the most unstable spin is flipped first. Each spin flip alters the exchange interaction on neighboring interface spins or adds new spins to the interface. Thus a single spin flip may produce a chain reaction. Once a spin is flipped it does not return to the unflipped state because the temperature is zero.

The overall advance of the interface is controlled by the value of the applied field H, which is varied quasistatically. It is initially taken to be the smallest value, H_0, that causes a single spin on the interface to flip. This single change in the spin array may cause neighboring spins to flip, which may induce further spin flips. The external field value is kept equal to H_0 until a stable interface is attained. Then H is increased so that a single spin flip occurs on the new interface, and the procedure is repeated until the interface attains the top of the array. As illustrated in Fig. 1, the value of H required for the pattern of flipped spins to span the system rapidly approaches a constant critical field H_C as $L \to \infty$.

It is convenient at this point to identify quantities that describe the importance of the local environment in producing spin flips. These will be useful in the discussion of the critical transitions below. Whether a spin s_i at the interface flips depends on the value of the external field H, the value of the local random field h_i, and the state of the z nearest-neighbor spins ($z = 3$, 4, and 6 for honeycomb, square, and triangular arrays). In contrast to the fluid invasion problem,[10] stability depends only on the number n of neighboring spins that are flipped and not on the relative positions of these spins. We show below that growth near the transition from faceted to fractal growth occurs entirely through flipping of spins

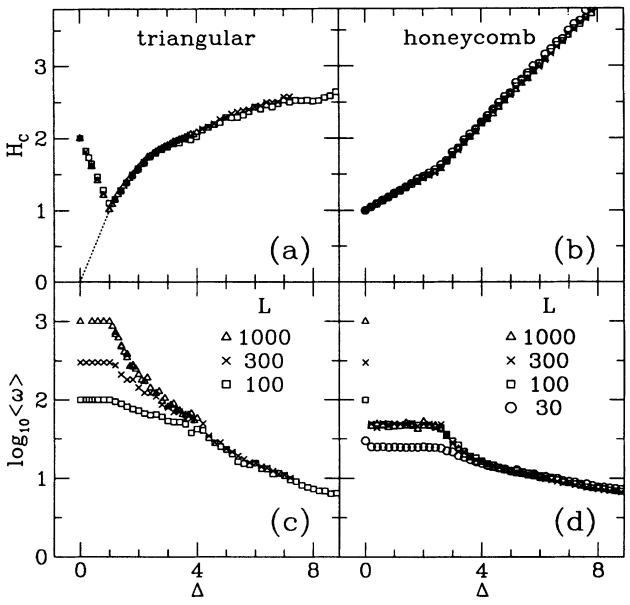

FIG. 1. Dependence of the average value of H needed to span the system (a) and (b) and the mean fingerwidth (c) and (d) on Δ in the triangular and honeycomb arrays. System sizes are indicated, and random fields were uniformly distributed between $\pm\Delta$. The dashed line in (a) indicates H_3^*, the top edge of the distribution function F_3.

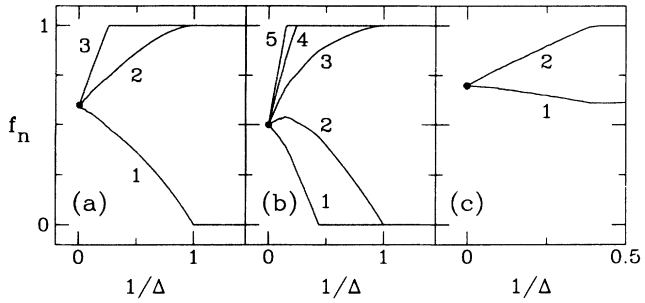

FIG. 2. Fraction f_n of spins with n flipped neighbors which will flip at H_C as a function of Δ. The curves give f_n for the indicated value of n in the (a) square, (b) triangular, and (c) honeycomb array for uniformly distributed random fields. Filled circles give the normal percolation concentration for each lattice.

with only two of the possible values of n.

The probability that a spin with n flipped neighbors becomes unstable at external field H is given by the distribution function $F_n(H) = P(z-2n-H)$. The fraction of unstable n-neighbor configurations at the critical field is then

$$f_n = \int_{-\infty}^{H_C} F_n(H)dH \quad . \tag{2}$$

In Fig. 2 we show the probabilities f_n, calculated as a function of Δ^{-1}, for uniform distributions of random fields in the square, triangular, and honeycomb lattices. We relate changes in these probabilities to changes in growth morphology in the following section.

III. RESULTS

A. Changes in growth morphology with disorder

The pattern of flipped spins depends strongly on the magnitude of the random fields.[9] In the limit of strong disorder, $\Delta >> 1$, the probability that a spin will flip becomes independent of its surroundings (i.e., n). The problem reduces to site percolation, and the patterns of flipped spins are self-similar structures characteristic of this model.[13,19] This limiting behavior is evident in Fig. 2. As $1/\Delta \to 0$, all f_n curves merge to the appropriate critical concentration for normal site percolation p_c. Values of p_c are 0.5, 0.5927, and 0.6962 in the triangular, square, and honeycomb lattices, respectively.[19]

As Δ decreases, the local environment becomes increasingly important in initiating spin flips. Spins with larger n are more and more likely to flip before other spins. This leads to cooperative invasion of neighboring regions, and the pattern of flipped spins becomes smoother. A measure of this change is given by the average fingerwidth $\langle\omega\rangle$ calculated as the mean width of segments of adjacent flipped spins.[7]

Figure 1(c) shows $\langle\omega\rangle$ versus Δ for spins on a triangular lattice with a uniform distribution of random fields. Similar results are obtained for the two other distributions. The increase in the fingerwidth as Δ decreases reflects a coarsening of the patterns. Results for three system sizes are presented, L =100, 300, and 1000. In all cases, $\langle\omega\rangle = L$ for $\Delta < \Delta_C = 1$. The same result was obtained for the square lattice in Refs. 9 and 10 and indicates that growth leads to a faceted pattern below this critical value of the randomness. Note in Fig. 1(a) that the critical field also shows a kink at Δ_C. The divergence of the fingerwidth in the $L \to \infty$ limit as Δ approaches Δ_C from above is discussed in Sec. III B.

Figures 1(b) and 1(d) show the dependence of H_c and $\langle\omega\rangle$ on Δ for spins on a honeycomb array with a uniform distribution of random fields. Note the striking difference between these results and those for the triangular and square lattices. While $\langle\omega\rangle$ initially increases as Δ decreases, it saturates for $\Delta < \Delta_0 \simeq 2.6$. There is a cusp in H_C at the same point. For large enough system sizes, the limiting value of $\langle\omega\rangle$ is near 50. Only for Δ exactly equal to zero does $\langle\omega\rangle$ jump discontinuously to L, indicating a faceted pattern in this isolated limit.

The dimensionality of patterns generated for different arrays and values of Δ was investigated through the box counting method.[13] System sizes from $L = 128$ to 2048 were used to identify and eliminate finite-size effects. For the honeycomb array we obtained a fractal dimension of $D_f = 1.89 \pm 0.01$ at $\Delta = 0.2$, 4, and 20. This indicates that the large-scale structure is characteristic of typical percolation patterns ($D_f = 91/48 \approx 1.896$) for all $\Delta > 0$. The cusps at Δ_0 in Figs. 1(b) and 1(d) merely reflect a freezing of the growth probabilities for $\Delta < \Delta_0$ (Fig. 2). This "frozen" regime is discussed further below. The same value of D_f was obtained for $\Delta > \Delta_C$ on the square and triangular lattices at length scales greater than the corresponding value of $\langle\omega\rangle$. For $\Delta < \Delta_C$ the patterns were two dimensional. In fact, *all* spins were flipped.

The transition to faceted growth and the value of Δ_C may be understood by considering the effect of local environment on growth in the triangular lattice. The starting interface for our simulations was chosen to be along a line connecting nearest-neighbor spins. Unflipped spins on the interface have $n = 2$ flipped spins and $z - 2 = 4$ unflipped spins as neighbors. The initial value of the external field in an infinite system is $H_0 = 2 - \Delta$, the lowest value at which a spin with $n = 2$ will flip. For finite systems, H_0 is slightly larger than this value.[9] Once the first spin above the original flat interface flips, two of its neighbors have equal numbers ($z/2 = 3$) of up and down spins as neighbors. For $\Delta < \Delta_C = 1$ these spins will also flip, since the maximum field required to flip a spin with $n = 3$ is $H_3^* = \Delta < H_0$. This changes the environment of two further spins to $n = 3$, and the process continues until all spins on the initial interface have flipped. Each row of spins then flips in turn until the interface reaches the top of the system. As a consequence, $H_C = H_0 = 2 - \Delta$ for $\Delta \leq \Delta_C$ and all spins in the system are flipped. A similar analysis in terms of spins with $n = 1$ and 2 applies to the square lattice.[9,10] Note that only the bounds of $P(h)$ are important, not the shape of the distribution. The value of $\Delta_C = 1$ is exact for any $P(h)$.

Growth from initial interfaces with different orienta-

tions depends on the boundary conditions. For example, we may start from an interface connecting second-neighbor spins on the triangular lattice, which is perpendicular to the interface discussed above. If periodic boundary conditions are imposed, growth can occur entirely through $n = 3$ processes and a chain reaction is produced for $H_C' = H_3^* = \Delta$ [dashed line in Fig. 1(a)]. If the system is terminated at the boundary, spins at the edges have $n = 2$ and will not flip at H_C'. This limits the chain reaction, and two facets connecting nearest-neighbor spins ($n = 2$) form. No further spin instabilities can occur until $H_C = 2 - \Delta$. At this field the facets grow to span the system. Similar behavior occurs for any other interface orientation on the triangular lattice and also on the square lattice.

No analog of the chain reaction leading to faceted growth can occur on the honeycomb lattice because the coordination number z is too small. Two orientations of the initial interface are shown in Fig. 3. There is no orientation where the interface spins always form unbroken chains of nearest neighbors. Thus, flipping a spin cannot lead to a chain reaction where all successive spins have a higher value of n. For orientation I_1, a spin flip produces two new neighbors that also have $n = 1$. For orientation I_2, one of the neighbors has $n = 2$, but flipping it adds a single spin with $n = 1$. Cooperative chain reactions, and thus faceted growth, are impossible. It is easy to see that faceted growth is only possible for $z \geq 2d$, where d is the spatial dimension. Only when this condition is met may each site have a neighbor in the preceding layer to initiate growth, an unbroken chain of nearest neighbors in each direction in the same layer, and a neighbor in the next layer to propagate the instability.

A surprising feature of the low disorder regime of the honeycomb array ($\Delta < \Delta_0$) is that the pattern of flipped spins is completely determined by the hierarchy of random-field values assigned to the lattice sites. If a pattern is generated for $\Delta < \Delta_0$, *exactly the same pattern* will be produced if all local-field values are scaled by a constant factor $\{h_i\} \rightarrow \{\sigma h_i\}$, with $0 < \sigma \leq \Delta_0/\Delta$. Therefore the plateaus in Fig. 1(d) actually represent a frozen state for all $0 < \Delta \leq \Delta_0$, and fluctuations are due to different realizations of the hierarchy of random fields.

Figure 2(c) reveals the origin of this frozen state. For $\Delta < \Delta_0$, all $n = 2$ processes lead to a spin flip ($f_2 = 1$).

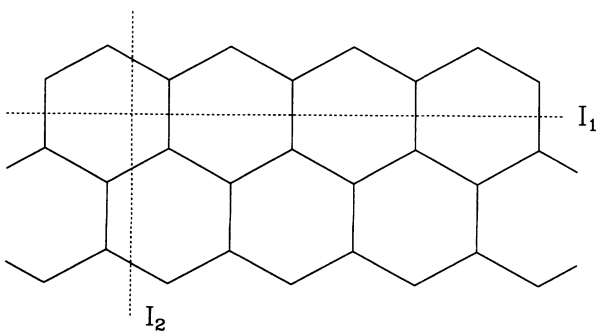

FIG. 3. Dashed lines indicate two possible orientations of the initial interface in the honeycomb lattice.

The invaded pattern is determined entirely by the set of spins that can flip with one flipped neighbor. Since only $n = 1$ configurations are important, the magnitude of the random fields relative to the exchange interaction is irrelevant. The fraction of spins with $n = 1$ that flip at H_C is a constant, $f_1 = 0.609 \pm 0.001$. This value of f_1 gives our most accurate determination of Δ_0. As Δ decreases to Δ_0, f_2 reaches 1. This implies that $H_C(\Delta_0) = \Delta_0 - 1$, which is the top of the distribution F_2. The value of Δ_0 is then determined by Eq. (2) and the value of f_1:

$$f_1 = \int_{1-\Delta_0}^{\Delta_0 - 1} P(1 - H)dH = \frac{1}{2} + \int_0^{\Delta_0 - 2} P(h)dh \ . \quad (3)$$

For the uniform distribution, $f_1 = 1 - 1/\Delta_0$, yielding $\Delta_0 = 2.588(7)$. For other distributions, $P(h)$ and Δ_0 are different. Equation (3) gives $\Delta_0 = 2.262(3)$ and 2.325(4) for linear and cosinusoidal distributions, respectively. The relation of this regime to bootstrap percolation is discussed in Sec. IV.

If a second-neighbor exchange coupling is included on the honeycomb array ($z \rightarrow 9$), the behavior becomes more like that on the square and triangular lattices. A transition from self-similar to faceted growth is found with decreasing randomness and is heralded by a power-law divergence of the fingerwidth. The peculiar frozen phase is completely eliminated. This indicates that this is not a "robust" regime and may be hard to produce experimentally.

B. The critical transition in square and triangular lattices

The critical transition from self-similar to faceted growth is identified by the divergence of the fingerwidth as Δ approaches Δ_C from above. Previous studies[9] of this divergence have focused on the exponent ν relating $\langle\omega\rangle$ to Δ:

$$\langle\omega\rangle \propto (\Delta - \Delta_C)^{-\nu} \ . \quad (4)$$

Different values for ν have been reported in the Ising[9] and fluid invasion[7,10] models. In this section we show that the divergence of $\langle\omega\rangle$ is most naturally described in terms of the probabilities f_n defined in Eq. (2) and plotted in Fig. 2.

Faceted growth occurs when all spins with $u = z/2$ flipped neighbors flip at a lower external field than any spins with $\ell = u - 1$ flipped neighbors. This implies that the probability distribution functions $F_u(H)$ and $F_\ell(H)$ do not overlap for $\Delta < \Delta_C$, and that H_C is in the gap between the two distributions (Fig. 1). Increasing the degree of randomness causes a relative displacement of these distributions until they touch ($\Delta = \Delta_C$) and overlap ($\Delta > \Delta_C$). As Δ increases from Δ_C, the probability f_u decreases from unity and f_ℓ increases from zero (Fig. 2). The total change in the two probabilities is bounded by the integral over the region where the corresponding distribution functions F overlap. If the tails of $P(h)$ go to zero as $(|\Delta| - |h|)^m$, then

$$(1 - f_u) + f_\ell \propto (\Delta - \Delta_C)^{m+1}. \quad (5)$$

For the uniform distribution $m = 0$, and for the cosinusoidal and linear distributions $m = 1$.

Figure 4 shows that there is a fixed relation between $1 - f_u$ and f_ℓ on the square lattice. Values were obtained analytically from H_C, which converges rapidly with increasing system size. Results for linear, uniform, and cosinusoidal distribution functions collapse onto a universal line. Only for $\Delta >> \Delta_C$, where other values of f_n begin to differ from 0 or 1, do the three curves separate. A similar universal line is found for the triangular lattice. The lines are well fit by power laws

$$(1 - f_u) \propto f_\ell^\beta \quad (6)$$

with $\beta = 1.82 \pm 0.05$ for the square lattice and 1.75 ± 0.05 for the triangular lattice.

The implication of Fig. 4 is that all distribution functions $P(h)$ produce the same family of percolation problems as $\Delta \to \Delta_C$ from above. The fingerwidth and all other characteristics of the pattern are specified entirely by either $1 - f_u$ or f_ℓ. In particular, we expect

$$\langle \omega \rangle \propto (1 - f_u)^{-\alpha} \quad (7)$$

near $f_u = 1$, where the value of α must be independent of $P(h)$. We have verified that plots of $\langle \omega \rangle$ against $1 - f_u$ at each L are indeed independent of the form of P. This allows us to focus our attention on a single case at the end of this section, the uniform distribution.

A simple "mean-field" estimate for α may be obtained by considering the growth process near Δ_C. The fingerwidth is infinite for $\Delta < \Delta_C$ because $f_u = 1$: A single spin flip causes an infinite chain reaction. For $\Delta > \Delta_C$ there is a probability $1 - f_u$ that each new spin on the interface that has $n = z/2$ will *not* flip. Any unflipped spin interrupts the chain reaction and leads to a finite fingerwidth. An estimate for $\langle \omega \rangle$ is given by the mean length of the chain reaction induced by a single spin flip on a flat interface. This length scales as $(1 - f_u)^{-1}$. The actual value of $\langle \omega \rangle$ should diverge at least as rapidly as this length, implying $\alpha \geq 1$.

In contrast to α, the exponent ν defined in Eq. (4) cannot be universal because the tails of the distribution function determine how rapidly $1 - f_u$ and f_ℓ vary with $\Delta - \Delta_C$. Indeed, we find that

$$f_\ell \propto (\Delta - \Delta_C)^{m+1}. \quad (8)$$

This is a direct consequence of Eq. (5) and the fact that $\beta > 1$. As $\Delta \to \Delta_C$, $(1 - f_u)/f_\ell \to 0$. Thus the value of H_C moves progressively closer to the top (Δ) of the distribution function F_u. The value of f_ℓ [Eq. (2)] can then be approximated by the integral of F_ℓ to Δ, which gives Eq. (8). Since $1 - f_u$ is smaller than f_ℓ and scales with a nontrivial exponent, we focus on it as the parameter controlling the fingerwidth and other properties of invaded patterns.

Figure 5 shows the dependence of $\log_{10}[1 - f_u]$ on $\log_{10}[\Delta - 1]$ (dashed lines) and $\log_{10}[1 - \Delta^{-1}]$ (solid lines). These results refer to the square lattice with uniform and cosinusoidal distributions of random fields, but similar results are obtained for the triangular lattice and for linear distributions of h. The figure indicates that a power-law relation,

$$(1 - f_u) \propto (\Delta - 1)^\mu \simeq (1 - \Delta^{-1})^\mu , \quad (9)$$

holds near $\Delta_C = 1$. While each pair of solid and dashed curves must have the same slope in this limit, the solid lines are straight over a wider range. This shows that $(1 - \Delta^{-1})$ is a better scaling variable than $(\Delta - 1)$, just as $(T - T_c)/T$ is a better scaling variable than $(T - T_c)/T_c$ for equilibrium transitions.[20] In the present context, this

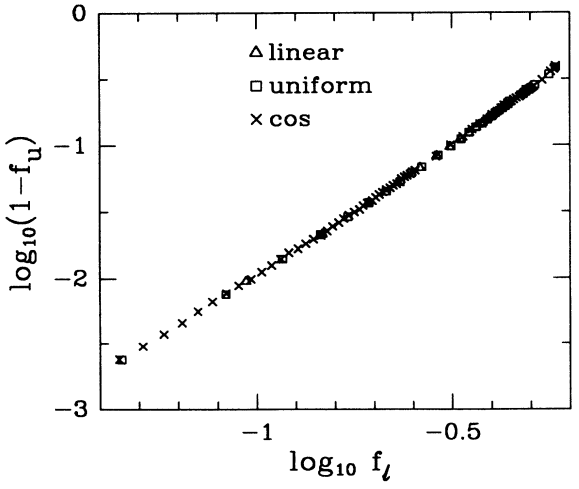

FIG. 4. Universal relation between the upper (f_u) and lower (f_ℓ) probabilities near the critical transition. Results are for the square lattice with the indicated distributions of disorder.

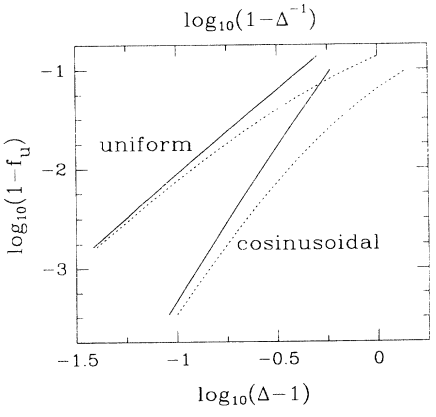

FIG. 5. Scaling of $1 - f_u$ with $\Delta - 1$ (dashed lines, bottom axis) and $1 - \Delta^{-1}$ (solid lines, top axis) near the critical point $\Delta_C = 1$ for the square lattice with uniform and cosinusoidal distributions of disorder. Each pair of solid and dashed curves shows the same asymptotic scaling, but the solid lines are straight over a wider range.

result may follow from the fact that all probability distributions introduced in Sec. II are proportional to $1/\Delta$.

Equations (6), (8), and (9) imply that $\mu = (m+1)\beta$. Numerical values of μ obtained directly by extrapolating the slope of Fig. 5 and related plots to $1 - f_u = 0$ are consistent with this relation. In particular, we find $\mu = 1.77 \pm 0.04$ and 1.69 ± 0.05 for uniform distributions on the square and triangular lattices, respectively. Results for linear and cosinusoidal distributions are less accurate because the curvature is greater. We find $\mu = 3.4 \pm 0.2$ and 3.3 ± 0.2 for square and triangular lattices, respectively. All our results are consistent with a common value of $\beta = \mu/(m+1) = 1.75 \pm 0.05$.

Determination of α and ν is more difficult because the fingerwidth is sensitive to finite-size effects. Since the relationship between $\langle\omega\rangle$ and $1 - f_u$ is found to be independent of the shape of the distribution function P, we focus on results for the uniform distribution. We have verified that results for other distributions give consistent values for the exponents.

To determine ν we use finite-size scaling. Based on the results for μ, we take $(\Delta - \Delta_C)/\Delta$ as the scaling variable and make the ansatz[9]

$$\langle\omega(L)\rangle = L\,\mathcal{F}[L^{1/\nu}(1 - \Delta^{-1})]. \tag{10}$$

Results were obtained for L between 30 and 1000 on the triangular lattice and 100 and 4000 on the square lattice. For uniform distributions of random fields, $\nu = 1.9 \pm 0.1$ provides a collapse of data for all system sizes on the square and triangular lattices.

This value of ν differs substantially from that reported in Ref. 9. There, $(\Delta - \Delta_C)/\Delta_C$ was taken as the scaling variable, and the largest system size was $L = 1000$. Using this scaling variable and including results for $L = 2000$ and 4000 produces a steady increase in the value of ν towards that quoted above. The large variation with system size in the effective value of ν for this scaling variable is also evident in the logarithmic derivative of $\langle\omega\rangle$ with respect to $(\Delta - 1)$. This direct determination of the effective exponent shows a steady increase from 1 to 1.8 as Δ decreases towards 1. As expected, the value of ν obtained with the scaling variable $(\Delta - \Delta_C)/\Delta$ changes more slowly with L. There is a small decrease in the corresponding logarithmic derivative from about 2.2 to 1.9 as $\Delta^{-1} \to 1$. Note that the limiting values of the logarithmic derivatives with respect to both scaling variables are consistent with our finite-size scaling determination of ν.

The quoted values of ν and μ for the uniform distribution imply $\alpha = \nu/\mu = \nu/[(m+1)\beta] = 1.09 \pm 0.09$. A lower bound on α is obtained by plotting $\langle\omega\rangle(1 - f_u)$ versus $(1 - f_u)$. This curve is monotonically decreasing, which implies $\alpha > 1$. Best fits to the logarithmic derivative in the region before finite-size effects enter give $\alpha = 1.1 \pm 0.1$, where the error bar reflects uncertainty in the fitting range. A finite-size scaling ansatz like that discussed above gives the same range of values. We thus conclude that the value of α is close to, but slightly larger than the mean-field value of unity.

IV. CONNECTION TO BOOTSTRAP AND DIFFUSION PERCOLATION

The growth model described here is closely related to a set of modified percolation models in which the occupation of a site depends on its environment.[15,16] In bootstrap percolation (BP), sites are initially occupied randomly with probability p. Then all sites that have fewer than m neighbors are successively removed (culled). The remaining occupied sites form the so-called infinite time limit cluster. For a given m, the critical probability p_c is defined as the value of p below which there is no infinite cluster in the infinite time limit. In diffusion percolation (DP), sites are *added* to the cluster if they have k or more neighbors. The $(z-m+1)$ DP problem is closely related to m-BP, since adding sites with at least $z - m - 1$ occupied neighbors involves removing unoccupied sites that have fewer than m unoccupied neighbors. However, the two processes are only equivalent on self-matching lattices.[15]

Our domain growth model is most closely related to DP. For $\Delta < \Delta_C$, any spin with $u = z/2$ flipped (occupied) neighbors will also flip ($f_u = 1$). As soon as any spins with $n < u$ can flip ($f_\ell > 0$), the entire system flips (fills). This is consistent with the fact that $p_c = 0$ for DP with $k = 2$ on the square lattice and $k = 3$ on the triangular lattice.[15] The corresponding BP problems have $p_c = 1$. This feature is easy to understand geometrically. For $m > 2$ BP on a square lattice, any void space (region of unflipped spins) is culled into a rectangular region that contains it.[15] For $p < 1$, voids of arbitrarily large linear dimensions occur in the initial set of occupied sites. Thus culling empties the entire lattice for $p < 1$. The same is true[15] in the triangular lattice for $m > 3$. Large voids are exponentially unlikely to occur in finite simulation arrays. Thus results for BP converge very slowly to the infinite sample limit [e.g., as $1/\ln L$ (Ref. 15)]. In our growth model, convergence is much more rapid because our starting interface spans the entire system in one direction. For example, the value of f_ℓ needed to fill the lattice scales as $L^{-0.8}$ on the square lattice.[9] This allows accurate studies of the model with relatively small system sizes.

We know of no previous studies of BP or DP on the honeycomb lattice. For $\Delta < \Delta_0$, our growth model corresponds to $k = 2$ DP, since $f_2 = 1$ (Fig. 2). The associated BP problem is $m = 2$. On most lattices $m = 2$ BP has the same p_c as normal percolation because only dangling ends of the infinite cluster are removed. However, our results indicate that $k = 2$ DP is different from normal percolation on the honeycomb lattice. We find that the threshold for an infinite cluster is $f_1 = 0.609 \pm 0.001$. This is substantially less than the upper bound provided by the threshold for normal percolation, $p_c = 0.6962$, and above the lower bound of $1/(z-1) = 0.5$ provided by mean-field theory.[19] It provides a new upper bound for p_c in $k = 2$ DP because growth is more difficult in our model. In the DP model, isolated sites and clusters are formed in the initial occupation of the lattice sites. These clusters may merge through flipping of intermediate spins to form an infinite cluster. Our growth model is more re-

strictive, since growth only occurs at the interface. Thus it cannot have a lower percolation concentration in the infinite sample size limit.

For $\Delta > \Delta_C$ or Δ_0, our model represents a continuous generalization of DP in which the influence of the environment is not decisive. Spins do not always flip when they have u flipped neighbors. Instead, they flip with probability f_u. As Δ increases further, other values of f_n begin to deviate from 1 or 0 (Fig. 2) and the problem becomes even richer.

One may readily construct more general Hamiltonians and distribution functions that produce arbitrary functions $F_n(H)$. For each, growth at a given H corresponds to a set of probabilities f_n. Figure 4 represents the reduced parameter space obtained if $f_3 = 1$ on the square lattice. The points map out the critical line in parameter space where infinite clusters first form. For smaller values of $f_\ell = f_1$ and $f_u = f_2$ (upper left of plot) growth is finite. For larger values, growth spans the system and is two dimensional.

The parameter space becomes three dimensional for $\Delta > 4$ on the square lattice because f_3 is no longer fixed at one. There is a critical surface in this three-dimensional space where infinite clusters appear. Different distribution functions $P(h)$ give different relations between f_1, f_2, and f_3 and thus pick out different points on this surface. Higher-dimensional critical surfaces and parameter spaces occur for the triangular lattice at large Δ.

In general, the maximum dimension of the effective parameter space is $z-1$ in our model because both f_z and f_0 are irrelevant: Flipping spins with z flipped neighbors only fills completely surrounded sites, and sites with no flipped neighbors are not on the interface. If spins away from the interface are allowed to flip the dimensionality of the space increases to z and the model becomes closer to BP.

V. CONCLUSIONS

The results presented in Sec. III show that the transition from fractal to faceted growth in domain-wall motion may be either first order, as on the honeycomb lattice, or second order, as on the square and triangular lattices. The exponents describing second-order transitions appear to be universal. One universal exponent, $\beta = 1.75 \pm 0.05$, describes the relation between the probability that a spin with $\ell = z/2 - 1$ flipped neighbors will flip at H_C and the probability that a spin with $u = z/2$ flipped neighbors will *not* flip (Fig. 4). A second, α, describes the divergence of the correlation length or fingerwidth as $1 - f_u$ goes to zero. Simulations give a value of $\alpha = 1.09 \pm 0.09$, which is close to the mean-field value of unity. The connection between domain growth and correlated percolation models discussed in Sec. IV may facilitate analytic calculations of the universal exponents describing domain growth. It also indicates that a new class of partially correlated percolation models (f_n not equal to 0 or 1) are physically relevant.

The relationship between $1-f_u$ and the strength of disorder is *not* universal. This explains why previous studies of fluid invasion[7,10] and domain growth[9] obtained different exponents ν for the divergence of $\langle\omega\rangle$ with changes in disorder or contact angle. From Eqs. (4)–(9) it is clear that the asymptotic value of ν only depends on the analytic form of the probability distribution functions for stability of local configurations of the interface. However, the numerical results presented here show that large system sizes are needed to see the asymptotic behavior.

The origin of faceted growth is the anisotropy in the array of spin sites. As a result, it is only observed in experiments on artificial anisotropic porous media, such as network models.[1] Real rocks and model bead packs do not have an underlying lattice structure and a different type of transition must occur with decreasing disorder or contact angle. Previous simulations on more complicated models of fluid invasion indicated that this is a transition from self-similar fractal growth to compact growth with a self-affine interface.[7,8] Subsequent experiments have confirmed that there is a sharp transition in growth morphology with decreasing contact angle[11] and experiments on wetting invasion of bead packs[21] and paper towels[22] clearly show that growth is self-affine. Moreover, the measured and calculated values of the associated roughness exponent are consistent.

These results are evidence for richer phase diagrams than those shown in Fig. 1, which contain a self-affine growth regime in addition to or instead of the faceted regime. It is not yet clear what features of the growth model are needed to produce this regime. Removing lattice anisotropy by using random spin or pore positions may be sufficient to introduce self-affine growth. However, this is not *required* because two models that have an underlying lattice produce self-affine interfaces: the fluid invasion model of Refs. 7 and 8, and domain growth in $3d$ random-field Ising models.[23] Future examination of models with different growth rules and of analogous lattice and continuum percolation problems may help to reveal the origin of self-affine growth.

ACKNOWLEDGMENTS

We thank N. Martys, V. Privman, and S.L.A. de Queiroz for useful discussions. Support from the National Science Foundation through Grant No. DMR-9110004 and from the Donors of The Petroleum Research Fund, administered by the American Chemical Society, is gratefully acknowledged. B.K. also acknowledges support from Conselho Nacional de Desenvolvimento Científico e Tecnológico (Brazil) and M.O.R. is grateful for the hospitality of the Theoretical Physics Institute at the University of Minnesota where this work was completed.

*On sabbatical leave from Departamento de Física, Pontifícia Universidade Católica do Rio de Janeiro, CEP 22453, Rio de Janeiro, Brazil.

†Present address: Physique de la Matière Condensée, College de France, 11, Place Marcelin-Berthelot, 75231 Paris CEDEX 05, France.

[1]R. Lenormand, J. Phys.: Condens. Matter **2**, SA79 (1990), and references therein.

[2]R. Bruinsma and G. Aeppli, Phys. Rev. Lett. **52**, 1547 (1984).

[3]J. Koplik and H. Levine, Phys. Rev. B **32**, 280 (1985).

[4]J. V. Maher, W. I. Goldburg, D. W. Pohl and M. Lanz, Phys. Rev. Lett. **53**, 60 (1984); D. A. Andelman and J. F. Joanny, in *Physics of Finely Divided Matter* (Springer-Verlag, Berlin, 1985), p. 361.

[5]M. O. Robbins and J. F. Joanny, Europhys. Lett. **3**, 729 (1987).

[6]J. P. Stokes, A. P. Kushnick, and M. O. Robbins, Phys. Rev. Lett. **60**, 1386 (1988).

[7]M. Cieplak and M. O. Robbins, Phys. Rev. Lett. **60**, 2042 (1988); Phys. Rev. B **41**, 11 508 (1990).

[8]N. Martys, M. Cieplak, and M. O. Robbins, Phys. Rev. Lett. **66**, 1058 (1991); Phys. Rev. B **44**, 12 294 (1991).

[9]H. Ji and M. O. Robbins, Phys. Rev. A **44**, 2538 (1991).

[10]B. Koiller, H. Ji, and M. O. Robbins, Phys. Rev. B **45**, 7762 (1992).

[11]A. P. Kushnick, J. P. Stokes, and M. O. Robbins, in *Fractal Aspects of Materials: Disordered Systems*, edited by D. A. Weitz, L. M. Sander, and B. B. Mandelbrot (Materials Research Society, Pittsburgh, 1988), p. 87; and (unpublished).

[12]J. P. Stokes, D. A. Weitz, J. P. Gollub, A. Dougherty, M. O. Robbins, P. M. Chaikin, and H. M. Lindsay, Phys. Rev. Lett. **57**, 1718 (1986); E. Peters and D. Flock, Soc. Pet. Eng. J. **21**, 249 (1981); R. L. Chuoke, P. van Meurs, and C. van der Poel, Trans. AIME **216**, 188 (1959).

[13]J. Feder, *Fractals* (Plenum, New York, 1988).

[14]R. Lenormand and S. Bories, C. R. Acad. Sci. Ser. B **291**, 279 (1980); R. Chandler, J. Koplik, K. Lerman, and J. F. Willemsen, J. Fluid Mech. **119**, 249 (1982).

[15]J. Adler and A. Aharony, J. Phys. A: Math. Gen. **21**, 1387 (1988); J. Adler, Physica A **171**, 453 (1991), and references therein.

[16]N. S. Branco, R. R. dos Santos, and S. L. A. de Queiroz, J. Phys. C **21**, 2463 (1988).

[17]S. Anderson and G. Mazenko, Phys. Rev. B **33**, 2007 (1986).

[18]G. Grinstein and S. Ma, Phys. Rev. B **28**, 2588 (1983).

[19]D. Stauffer, *Introduction to Percolation Theory* (Taylor and Francis, London, 1985).

[20]A. Aharony and M. E. Fisher, Phys. Rev. Lett. **45**, 679 (1980).

[21]M. A. Rubio, C. Edwards, A. Dougherty, and J. P. Gollub, Phys. Rev. Lett. **63**, 1685 (1989); **65**, 1389 (1990); V. K. Horváth, F. Family, and T. Vicsek, Phys. Rev. Lett. **65**, 1388 (1990); J. Phys. A **24**, L25 (1991); P.-z. Wong (private communication).

[22]S. V. Buldyrev, A.-L. Barabási, F. Caserta, S. Havlin, H. E. Stanley, and T. Vicsek, Phys. Rev. A **45**, 8313 (1992).

[23]H. Ji and M. O. Robbins (unpublished).